Topological Gauge Structure and Phase Diagram of a Doped Antiferromagnet

Su-Peng Kou[1] and Zheng-Yu Weng[2]

[1] *Department of Physics, Beijing Normal University, Beijing, 100875, China*
[2] *Center for Advanced Study, Tsinghua University, Beijing, 100084, China*

We show that a topological gauge structure in an effective description of the t-J model gives rise to a global phase diagram of antiferromagnetic (AF) and superconducting (SC) phases in a weakly doped regime. Dual confinement and deconfinement of holons and spinons play essential roles here, with a quantum critical point at a doping concentration $x_c \simeq 0.043$. The complex experimental phase diagram at low doping is well described within such a framework.

PACS numbers: 74.20.Mn, 74.25.Ha, 75.10.-b

Introduction. Cuprate superconductors have shown different ordering tendencies as the hole concentration x varies [1, 2, 3, 4]. The parent state is a Mott insulator with an AF long range order (AFLRO). Hole doping leads to the disappearance of AFLRO at $x_0 \sim 0.02$. In a lightly doped region, $x_0 < x < x_c \sim 0.05$, the low temperature (T) state is a cluster spin-glass phase with localized holes. At $x > x_c$, the holes are delocalized and the ground state becomes a d-wave SC phase.

In literature, based on the three-band model, dipole defects induced by holes have been conjectured [5, 6, 7] as responsible for the destruction of the AFLRO as well as the spin-glass phase [8]. A different cause for destroying the AFLRO has been attributed [9] to holes dressed with vortices [10]. But a systematic model study is still lacking, which prevents us to fully understand the evolution of the AF and SC phases at low doping.

Theoretically, the single-band $t-J$ model has been widely used to describe electronic properties in cuprates. But it is notably difficult to conduct a reliable investigation continuously going from half-filling to a superconducting phase. Thus, a tractable model of the doped AF-Mott insulator is called for. Such a model should well describes antiferromagnetism at half-filling, on one hand, and give rise to a d-wave superconductivity at large doping, on the other hand, while the Hilbert space remains restricted with x as the *natural* charge carrier concentration.

An effective description which satisfies the above criteria has been derived [11] from the t − J Hamiltonian based on the bosonic resonating-valence-bond (b-RVB) pairing [12, 13]. It is given by $H_{string} = H_h + H_s$ with

$$H_h = -t_h \sum_{\langle ij \rangle} (e^{iA^s_{ij} - i\phi^0_{ij}}) h^\dagger_i h_j + H.c. \quad (1)$$

$$H_s = -J_s \sum_{\langle ij \rangle \sigma} (e^{i\sigma A^h_{ij}}) b^\dagger_{i\sigma} b^\dagger_{j-\sigma} + H.c. \quad (2)$$

Here h_i and $b_{i\sigma}$ are *bosonic* holon and spinon operators, respectively. At half-filling, H_h is absent while H_s reduces to the Schwinger-boson mean-field Hamiltonian [13] ($A^h_{ij} = 0$), which correctly characterizes AF correlations. In particular, a *spinon* Bose condensation, $< b_{i\sigma} > \neq 0$, leads to an AFLRO. On the other hand, when *holons* are Bose condensed at *large* doping, the ground state becomes a d-wave SC [11, 14]. *Without* considering the spinon condensation, such a phase would extrapolate at $x \to 0$ with $T_c \to 0$. But at low doping, spins can still remain ordered. It thus may push the SC phase boundary to a finite x_c, leaving a region for a rich competing phenomenon.

In this Letter, we explore such a regime lying between the half-filling antiferromagnetism and the superconducting phase. We find that the theoretical phase diagram bears striking similarities to the experimental one, and is controlled by a dual confinement-deconfinement procedure determined by the topological gauge structure in (1) and (2).

Topological gauge structure. The nontriviality of H_{string} arises from the link variables, A^s_{ij} and A^h_{ij}, in the doped case. These link variables satisfy topological conditions: $\sum_c A^s_{ij} = \pm\pi \sum_{l\in c}(n^s_{l\uparrow} - n^s_{l\downarrow})$ and $\sum_c A^h_{ij} = \pm\pi \sum_{l\in c} n^h_l$ for a closed loop c (here $n^s_{l\sigma}$ and n^h_l denote spinon and holon number operators, respectively). So A^s_{ij} reflects the frustrations of spin background on the kinetic energy of charge degrees of freedom, while A^h_{ij} represents the influence of charge part on spin degrees of freedom. [ϕ^0_{ij} in (1) describes a uniform π flux per plaquette with $\sum_\Box \phi^0_{ij} = \pm\pi$].

It has been previously shown [14] that in the superconducting state with a holon Bose condensation, spinons are "confined", due to the gauge field A^s_{ij}, to form integer spin excitations and nodal quasiparticles emerge as recombined holon-spinon composites. The deconfinement of spinon pairs occurs at $T \geq T_c$, which is responsible for destroying the SC phase coherence. In the following, we show that when spinons are condensed, holons will be "confined" too, due to the gauge field A^h_{ij}.

Holon confinement. If spinons are condensed, it is straightforward to observe that a holon will cost a logarithmically divergent energy in H_s. Using an expansion $e^{i\sigma A^h_{ij}} \simeq 1 + i\sigma A^h_{ij} - (A^h_{ij})^2/2$, the energy cost of a holon in H_s can be estimated as

$$\Delta E_s \sim J_s < b^\dagger >< b^\dagger > \sum_{\langle ij \rangle} (A^h_{ij})^2 \sim J_s \ln(L/a), \quad (3)$$

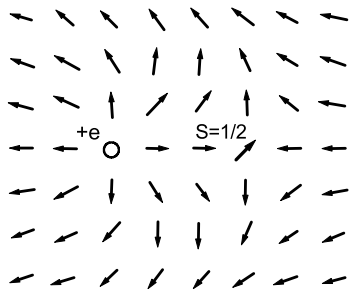

FIG. 1: In the spinon Bose condensed phase, a holon-meron is confined with an antimeron to form a hole-dipole composite, which carries a charge +e and spin 1/2. The arrows denote $\mathbf{n}_i \propto (-1)^i \langle \mathbf{S}_i \rangle$

where L is the size of the sample and a is lattice constant. Such an infinite energy can be physically understood as follows. In terms of the spin flip operator [11]

$$S_i^+ = (-1)^i b_{i\uparrow}^\dagger b_{i\downarrow} \exp\left[i\Phi_i^h\right], \tag{4}$$

the spin polarization $\left\langle S_i^+ \right\rangle$ is twisted away from the Néel order $(-1)^i < b_{i\uparrow}^\dagger >< b_{i\downarrow} >$ by an angle $\Phi_i^h = \sum_{l\neq i} \mathrm{Im}\ln(z_i - z_l)\, n_l^h$, which has a "meron" configuration as $\Phi_i^h \rightarrow \Phi_i^h \pm 2\pi$ by going around a holon once. In other words, a holon defined here is a topological object carrying a spin-meron twist. *So a single holon will not appear in the low-energy spectrum and must be confined in the spin ordered phase.*

It is easy to show that two holons will *repulse* each other logarithmically in H_s as they are merons of the *same* topological charge [15]. The only way to realize a finite-energy *hole* object in the present framework is for each holon-meron to "nucleate" an anti-meron from the vacuum. Such an anti-meron corresponds to a twist

$$< b_{i\sigma} >\rightarrow< \bar{b}_{i\sigma} > \exp\left[i\frac{\sigma}{2}\mathrm{Im}\ln(z_i - z_0)\right], \tag{5}$$

with z_0 denoting its position. Then, the meron twist Φ_i^h in $\left\langle S_i^+ \right\rangle$ or the link variable A_{ij}^h in ΔE_s will be canceled out by the corresponding anti-merons if z_0's approaches to the holon positions. Each doped hole will then behave like a *dipole* composed of a confined pair of meron (holon) and anti-meron as shown in Fig. 1.

The total energy of a dipole can be generally written by [15]

$$E_{dipole} = E_{\rm core}^h + E_{\rm core}^m + V, \tag{6}$$

where the infinite energy in Eq. (3) is replaced by a finite one

$$V(|\delta\mathbf{R}|) = \Delta E_s \sim J_s \ln(|\delta\mathbf{R}|/a), \tag{7}$$

in which $\delta\mathbf{R}$ denotes the spatial separation of two poles of the dipole. Here $E_{\rm core}^h$ and $E_{\rm core}^m$ represent, respectively, the core energies of a holon-meron and an anti-meron [$E_{\rm core}^h$ also includes the hopping energy from (1)].

Therefore, a holon must be confined to an anti-meron to form a hole-dipole object in the spin ordered phase. Note that a dipolar result was first found by Shraiman and Siggia [16] based on a semi-classical treatment of the $t-J$ model. But there is an important difference: in the present case the hole sits at a *pole* instead of the *center* of a dipole as shown in Fig. 1. A more detailed and elaborate discussion on physical properties of hole-dipoles in the spinon condensed phase is given elsewhere [15].

Quantum critical point (QCP) x_c. The holon confinement holds only at low doping. With the increase of x, as more and more hole-dipoles are present at $T=0$, the "confining" potential (7) can get fully screened for large pairs of meron and anti-meron, leading to a topological transition at $x = x_c$, from dipoles to free merons in a fashion of the Kosterlitz-Thouless (KT) transition [17].

We shall employ a standard KT renormalization group (RG) method to calculate x_c. For this purpose we rewrite interaction $V(r)$ in (6) as $2\pi\beta^{-1}K\ln(r/a)$, where the reduced spin stiffness $K(a) \propto J_s\beta$ ($\beta = 1/T$). The probability of creating a meron-antimeron pair with two poles separated by a distance a is given by the pair fugacity $y^2(a)$. Note that in the conventional KT theory, $y^2(a) = e^{-\beta(E_{\rm core}^h + E_{\rm core}^m)}$, but in the present case the dipole number is *fixed* at x per site and thus the initial $y^2(a)$ must be adjusted accordingly (see below).

In the RG scheme, small pairs of sizes within r and $r+dr$ are integrated out starting from the lattice constant $r = a$. The renormalization effect is then represented by renormalized quantities $X(r) \equiv \frac{1}{K(r)}$ and $y^2(r)$, which satisfy the famous recursion relations [17, 18]

$$dy^2/dl = 2(2 - \frac{\pi}{X})\, y^2, \tag{8}$$

$$dX/dl = 4\pi^3 y^2, \tag{9}$$

where $r = ae^l$. What makes the present approach different from the conventional KT theory is the presence of a finite density of the hole-dipoles even at $T=0$ as pointed out above. Here, by noting $\frac{y^2(r)}{r^4} d^2\mathbf{r}$ as the areal density of pairs of sizes between r and $r+dr$ [17], we have the following constraint

$$\begin{aligned} x/a^2 &= \int_a^\infty dr\, 2\pi r\, \frac{y^2(r)}{r^4} \\ &= \frac{1}{2\pi^2 a^2} \int_0^\infty dl e^{-2l}\, \frac{dX}{dl}\ , \end{aligned} \tag{10}$$

In obtaining the second line the recursion relations (8) and (9) are used.

The RG flow diagram of (8) and (9) is well known: the two basins of attraction are separated by the initial values which flow to $X^* = \pi/2$ and $y^* = 0$ in the limit

$l \to \infty$. For $T \to 0$, $X(l=0) \to 0$, the separatrix of the RG flows is given by

$$l = \int_0^X \frac{dX'}{4(X' - \pi/2) - 2\pi \ln(2X'/\pi)}, \qquad (11)$$

and the critical hole density can be numerically determined in terms of (10) and (11) as

$$x_c \simeq \frac{0.84}{2\pi^2} = 0.043. \qquad (12)$$

Therefore, a QCP is found at x_c where hole-dipoles dissolve into holon-merons and antimerons. At $x < x_c$, since the fugacity y is always renormalized to zero, each holon-meron has to be bound to an immobile antimeron, implying that the doped holes should be self-trapped in space [15].

Disappearance of AFLRO. Even in the confined phase, $x < x_c$, the system is not necessarily always AF ordered. The presence of hole-dipole can lead to the destruction of the true AFLRO before reaching x_c. The basic physics reason is due to the fact that dipoles have a long-range effect ($\frac{1}{r}$) on the distortion of the magnetization direction.

Let us introduce a unit Néel vector $\mathbf{n}_i \propto (-1)^i \langle \mathbf{S}_i \rangle$. Define $n_i^x + i n_i^y \equiv e^{i\phi_i + i\phi_0}$, with $\mathbf{n}_0 = (\cos\phi_0, \sin\phi_0)$ as the global AF magnetization direction. Then a hole-dipole centered at the origin [Fig. 1] will give rise to

$$\phi_i \simeq (\mathbf{p} \cdot \mathbf{r}_i)/|\mathbf{r}_i|^2 \qquad (13)$$

at $|\mathbf{r}_i| >> |\mathbf{p}|$, with $\mathbf{p} \equiv -\hat{\mathbf{z}} \times \delta\mathbf{R}$.

The twist of the Néer vector due to a dipole at the original is given by $\delta\mathbf{n}_i = \mathbf{n}_i - \mathbf{n}_0 \approx \mathbf{m}\phi_i$, with the unit vector $\mathbf{m} = (-\sin\phi_0, \cos\phi_0)$. In the continuum limit, $\nabla^2 \mathbf{n}(\mathbf{r}) = 2\pi \mathbf{m} (\mathbf{p} \cdot \nabla) \delta(\mathbf{r})$. The multi-dipole solution can be generally written as $\nabla n^\mu(\mathbf{r}) = 2\pi \sum_l \mathbf{p}_l \delta(\mathbf{r} - \mathbf{r}_l) m_l^\mu + \mathbf{g}_\perp^\mu$ where l denotes the index of hole-dipoles and $\nabla \cdot \mathbf{g}_\perp^\mu = 0$. The transverse component $\mathbf{g}_\perp^\mu$ will have no effect in the nonlinear sigma model [7] and we may only focus on the longitudinal part of $\nabla n^\mu(\mathbf{r})$ below. At low temperature, we may assume that the hole-dipoles are localized and treat all the variables, $\mathbf{m}_l$, $\mathbf{p}_l$, and $\mathbf{r}_l$, as quenched. Defining the quenched average $\langle \cdots \rangle_q$, and using $\left\langle m_l^\mu m_{l'}^\nu \right\rangle = 1/2 \delta_{\mu\nu}\delta_{ll'}$, $\left\langle p_l^i p_{l'}^j \right\rangle = \delta_{ij}\delta_{ll'}\eta a^2/2$ with $\eta = \left\langle |\delta\mathbf{R}|^2 \right\rangle_q / a^2$, we get

$$\left\langle \partial_i n^\mu(\mathbf{r}) \partial_j' n^\nu(\mathbf{r}') \right\rangle_q = \upsilon \delta_{ij} \delta_{\mu\nu} \delta(\mathbf{r} - \mathbf{r}') \qquad (14)$$

in which $\upsilon = Ax$, with $A = \pi^2 \eta$.

The RG study of the non-linear sigma model with quenched random dipole moments has been given [7] within a one-loop approximation. Even though the origin of the dipole moments is different, once (14) is determined, these results can be directly applied here. The AF correlation length ξ has been obtained at low T as $\xi/a \simeq \exp(\frac{2\pi}{3\upsilon})$. The Néel temperature $T_N(x)$ is roughly given by the solution of $\alpha\xi^2 \simeq a^2$,where $\alpha \sim 10^{-5}$ [1], representing the effect of the interlayer coupling $J_\perp/J$. Then the critical doping x_0 at which the AFLRO disappears can be estimated by $x_0 = -\frac{4\pi}{3A \ln\alpha}$. In order to get the experimental value $x_0 \sim 0.02$, it has been assumed $A \sim 20$ in Ref. [7]. In the present case, a self-consistent calculation leads to $\eta = 1.23$ and $x_0 \simeq 0.03$, determined by the KT theory based on (8) and (9). On the other hand, at $x \to 0$ where $\upsilon \ll t \equiv T_N/\rho_s$ ($\rho_s \sim 0.176J$ is the spin stiffness [13]), $\xi/a \sim \exp(\frac{2\pi}{3\upsilon}[1-(1-\frac{\upsilon}{t})^3])$ [7] and one obtains $T_N(x) \approx T_N(0) - Ax\rho_s$, with $T_N(0) = -\frac{4\pi}{\ln\alpha}\rho_s$. The plot of T_N as a function of x is shown in Fig. 2.

In Fig. 2, a characteristic temperature T_f in the AFLRO phase is also shown by the dotted curve, which represents the fact that although the holes are all localized, the directions of their dipole moments can still rotate freely to reach annealed equilibrium above T_f. The dipole–dipole interaction causes an energy difference of two dipoles, from parallel to perpendicular in their relative moment alignment, is proportional to $1/r^2$ (r is the spatial separation between them). Associating r with the average hole-hole distance: $r = a/\sqrt{x}$, the interaction energy then scales linearly with x, such that $T_f \sim 1/r^2 \sim x$ [5, 19]. In the region $x_0 < x < x_c$, the AFLRO is destroyed and the AF orders are limited mainly by finite size effects, where the size of the AF domains is determined by hole concentration, $\xi \sim a/\sqrt{x}$. The spin-glass freezing temperature is then expected to vary as $T_g \sim \xi^2 \sim 1/x$. Such a phase has been known as a cluster spin glass [8]. Below the temperature T_g the hole-dipolar configurations form a glass and their dynamics strongly slows down.

Superconducting phase. At $x \geq x_c$, holons are deconfined and free, and thus will experience Bose condensation at low T, giving rise [11, 14] to a d-wave superconducting ground state.

We have shown that the holons are confined to form immobile dipoles at $x \leq x_c$, instead of being Bose condensed. At $x = x_c$, the concentration of anti-merons is x_c, while at $x \gtrsim x_c$,, for each additional holon, there will be no more anti-meron to be created so that the concentration of anti-merons is roughly fixed at x_c until $<| b_{i\sigma} |> = 0$. Thus, in an overlap regime of $<| b_{i\sigma} |> \neq 0$ and $< h_i > \neq 0$ at $x \gtrsim x_c$, A_{ij}^h in H_s should be replaced by a $\tilde{A}_{ij}^h$ due to the presence of antimerons, and its strength $\tilde{B}^h = \pi x_{eff}/a^2$ is now controlled by an effective concentration $x_{eff} = x - x_c$, instead of x itself. Eventually at higher doping, $<| b_{i\sigma} |> = 0$ with no more (anti)merons, one will recover x from x_{eff} as the parameter representing the doping effect on the SC properties [11].

At small doping, the continuum version of (2) is a CP^1 [20] model, which leads to the Klein-Gordon equation: $\left(\partial_i + i\tilde{A}_i^h \sigma\right)^2 z^\sigma = (E/c_s)^2 z^\sigma$, where $z^\sigma = \frac{1}{2}(\bar{b}_{A\sigma} + \bar{b}_{B\sigma}^*)$, $\bar{b}_{A\sigma}$ and $\bar{b}_{B\sigma}$ are spinons on A and on B sublattices, and c_s is the effective spin-wave velocity ($c_s \sim$

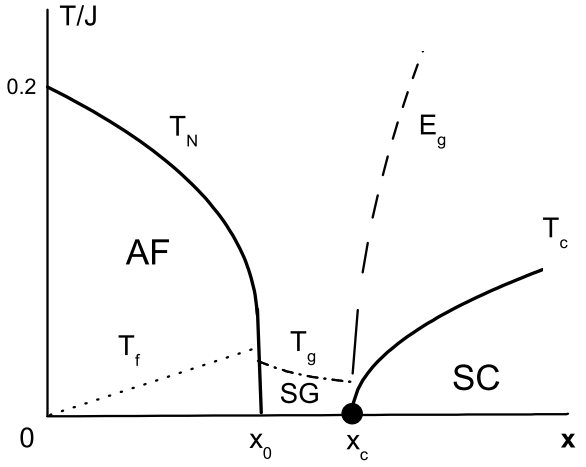

FIG. 2: Phase diagram at low doping x : a dual confinement-deconfinement occurs at a quantum critical point $x_c \simeq 0.043$. The Néel temperature T_N vanishes at $x_0 \simeq 0.03$. T_f and T_g denote characteristic spin freezing temperatures, and T_c is the superconducting transition temperature. E_g is a characteristic spin energy (see text).

$1.64aJ$ [13]). The energy spectrum is [21, 22] $E_{n,m} = \pm c_s\sqrt{(n+1/2+\mid m\mid \mp m)\tilde{B}^h}$ and the wave functions are $z^{\sigma}_{n,m} \sim \rho^{|m|}e^{im\varphi}F(-n,\mid m\mid +1,\alpha^2\rho^2)\exp(-\alpha^2\rho^2/2)$, where F is the hypergeometric function, m is the eigenvalue of the angular momentum, and n is the eigen-value of the harmonic oscillation level number, $\alpha^2 = \tilde{B}^h/2$, $\rho = \sqrt{x^2+y^2}$. The energy gap between first excited state and the ground state is

$$E_s = E_1 - E_0 \sim 1.5J\sqrt{x_{eff}}. \qquad (15)$$

This result is in contrast to $E_s \propto xJ$ $(x \to 0)$ obtained at $<|b_{i\sigma}|>= 0$ [11]. The characteristic spin energy is then given by $E_g \sim 2E_s$. It has been previously established [23, 24] that the superconducting transition occurs when spinons become deconfined at a finite temperature, which is determined at $T_c \simeq \frac{E_g}{c}$ with $c \sim 4$, as shown in Fig. 2.

In conclusion, the low-temperature phase diagram for a doped Mott antiferromagnet described by (1) and (2) is basically determined by its intrinsic topological gauge structure. A quantum critical point at $x_c \simeq 0.043$ is found, below and above which, *dual confinement and deconfinement* take place at $T = 0$, leading to a systematic evolution from the antiferromagnetic to superconducting phases as a function of x. The complex experimental phase diagram in the weakly doped cuprates may be understood within such a framework. For example, the *dipolar* effect of doped holes is responsible for a vanishing T_N at $x_0 \sim 0.03$ and a cluster spin-glass phase at $x_0 < x < x_c$. The superconducting state sets in at $x \geq x_c$, whose phase coherence is destroyed by a deconfinement of spinons at $T \geq T_c$ [23, 24]. Due to the space limit, we have not discussed the possible stripe instability in the same model, which is explored at low doping as a competing phenomenon elsewhere [15].

Acknowledgments

We thank T. Li and H.T. Nieh for helpful conversations. S.-P.K. is partially supported by the NSFC Grant no. 10204004. Z.-Y.W. acknowledges partial support from NSFC Grant no. 90103021 and no. 10247002.

[1] B. Keimer, *et al.*, Phys. Rev. B**46**, 14034 (1992).
[2] F. C. Chou, *et al.*, Phys. Rev. Lett. **71**, 2323 (1993).
[3] Ch. Niedermayer, *et al.*, Phys. Rev. Lett. **80**, 3843 (1998).
[4] A. Ino, *et al.*, Phys. Rev. B**62** , 4137 (2000).
[5] A. Aharony *et al.*, Phys. Rev. Lett. **60**, 1330 (1988).
[6] L. I. Glazman and A. S. Ioselevich, Z. Phys. B**80**, 133 (1990).
[7] V. Cherepanov, *et al.* cond-mat/9808235; I. Y. Korenblit, *et al.*, cond-mat/9709056.
[8] K.S.D. Beach, R.J. Gooding, cond-mat/0001095.
[9] C. Timm and K.H. Bennemnn, Phys. Rev. Lett. 84, 4994 (2000)
[10] J.A. Verges *et al.,* Phys. Rev. B**43,** 6099 (1991); M. Berciu and S. John, Phys. Rev. B**59**, 15143 (1999).
[11] Z. Y. Weng, *et al.*, Phys. Rev. B**55**, 3894 (1997); Z. Y. Weng, *et al.*, Phys. Rev. Lett. **80**, 5401 (1998).
[12] S. Liang, *et al.*, Phys. Rev. Lett., **64**, 365 (1988).
[13] D.P. Arovas and A. Auerbach, Phys. Rev. B**38**, 316 (1988).
[14] Y. Zhou, *et al.*, Phys. Rev. B **67**, 064512 (2003).
[15] S.P. Kou and Z.Y. Weng, Phys. Rev. B **67**, 115103 (2003).
[16] B. Shraiman and E. Siggia, Phys. Rev. Lett. **61**, 467 (1988).
[17] J.M. Kosterlitz and D.J. Thouless, J. Phys. C **6**, 1181 (1973); J.M. Kosterlitz, *ibid.* **7**, 1046 (1974).
[18] P.M. Chaikin and T.C. Lubensky, *Principles of Condensed Matter Physics* (Cambridge university press, 1995), p.547.
[19] R.J. Gooding, N.M. Salem, A. Mailhot, cond-mat/9312082.
[20] N. Read and S. Sachdev, Phys. Rev. Lett. **62**, 1694 (1989).
[21] L.D. Landau and E.M. Lifshitz, *Quantum Mechanism* (Pergamon, New York, 1976), p.457.
[22] A. Auerbach, *et al.*, Phys. Rev. B**43**, 11515 (1991).
[23] Ming Shaw, *et al.*, cond-mat/0110527.

[24] V. N. Muthukumar and Z. Y. Weng, Phys. Rev. B**65,** 174511 (2002).